Journal of Applied Polymer Science

# Composite Materials of Graphene Nanoplatelets and Polypropylene, Prepared by *In Situ* Polymerization

**Sergey V. Polschikov,[1] Polina M. Nedorezova,[1] Alla N. Klyamkina,[1] Anton A. Kovalchuk,[1] Alexander M. Aladyshev,[1] Alexander N. Shchegolikhin,[2] Vitaliy G. Shevchenko,[3] Vyacheslav E. Muradyan[4]**

[1]N.N. Semenov Institute of Chemical Physics, Russian Academy of Sciences, Moscow, Russia
[2]N.M. Emmanuel Institute of Biochemical Physics, Russian Academy of Sciences, Moscow, Russia
[3]N.S. Enikolopov Institute of Synthetic Polymer Materials, Russian Academy of Sciences, Moscow, Russia
[4]Institute of the Problems of Chemical Physics, Russian Academy of Sciences, Chernogolovka, Russia

Correspondence to: V. G. Shevchenko (E-mail: shev@ispm.ru)

**ABSTRACT:** Nanocomposites of polypropylene and graphene nanoplatelets were synthesized by *in situ* polymerization in liquid monomer in the presence of highly effective isospecific homogeneous metallocene catalyst. Microstructure, mechanical, dielectric, and thermal properties of composites are presented. X-ray phase analysis data indicate that graphene nanoplatelets are present in composites as thin flaky particles aggregates, with aspect ratio affected by sonication of reaction mixture. Crystallization temperature of polypropylene increases in composites. Nanocomposites are characterized by high rigidity, thermal stability, and crystallization temperature, low conductivity, and high dielectric losses in the microwave range. © 2012 Wiley Periodicals, Inc. J. Appl. Polym. Sci. 000: 000–000, 2012

**KEYWORDS:** nanocomposites; graphene nanoplatelets; poly(propylene); metallocene catalysts

Received 11 March 2010; accepted 30 March 2012; published online
**DOI: 10.1002/app.37837**

## INTRODUCTION

Multifunctional polymer composites with nanosized fillers are now the subject of intense research. Relatively small concentrations of nanoparticles in polymer matrix (below 2.5 vol %) produce better results compared with traditional particles-filled composites. Among the promising fillers for polymer nanocomposites, there is a choice of different carbon allotropes and nanostructures: fullerenes, carbon nanotubes (CNT), nanofibers, and graphene. The combination of structural, mechanical, and electrophysical properties of these fillers provides composites possessing simultaneously the whole complex of important properties: higher mechanics, enhanced electrical and thermal characteristics, and flame-retardant properties.

Until recently, CNT were dominant nanosized carbon fillers for polymer composites. However, effective utilization of CNT is hindered by the complexity of their dispersion in polymer matrix and high cost. One of the alternatives is graphene, the material, which has become one of the hottest topics in physics and materials science.[1] Graphene, with its unique physical properties[2] is multifunctional filler that can improve electrical, thermal, mechanical, or gas barrier properties of polymers at extremely small loading.

Graphene is two-dimensional allotrope of carbon, formed by single layer of carbon atoms, bonded by $sp^2$ orbitals into hexagonal two-dimensional crystal lattice. Besides these ideal structures, controlled reduction of graphite oxide yields reduced graphene oxide sheets, which contain a few layers of graphene. The structures with several (2–5) layers of carbon atoms are also named graphene nanoplatelets (GNP). They are much easier to produce, compared with CNT and controlled reduction allows preparing nanoplatelets with different oxidation levels and different electronic properties.

The paper reports the synthesis and properties of composite materials, made from isotactic polypropylene (IPP) and GNP by *in situ* polymerization method. Existing methods of preparing polymer composites with nanosized carbon fillers provide acceptable dispersion of filler mainly in the case of mixing in solution and subsequent casting of film.[3] Melt mixing gives reduced dispersion degree resulting in poorer mechanical and transport properties. *In situ* polymerization provides the advantages of

solvent processing for polymers that cannot be processed in solution. The results are compared with the properties of similar composites, containing multiwalled CNT (MWCNT).[4,5]

## EXPERIMENTAL

### Preparation and Characterization of Filler–GNP

GNP were prepared by chemical oxidation of graphite and its subsequent reduction.[6] Graphite oxide was made by modified method of Hummers and Offeman[7]: oxidation of graphite by $KMnO_4$ in concentrated $H_2SO_4$.[8] Aqueous suspension of graphite oxide was reduced by hydrazine hydrate with ultrasonic treatment at 70°C for 4 h and subsequent boiling during 2 h. Reduced GNP powder was washed in bidistilled water, freeze-dried and then heated in argon flow at 900°C for 1 h.

Electronic microphotographs of GNP (Figure 1) were taken with scanning electronic microscope JSM-5300LV (Jeol). X–ray phase analysis of GNP powder was made with diffractometer ADP-1 (monochrome Cu-$K_\alpha$ radiation). Interlayer distance was calculated from the Scherrer equation: $d_{002} = \lambda/2 \times \sin \theta_{002}$, where $\lambda$ is the wavelength of Cu-$K_\alpha$ radiation, $\theta$ is dispersion angle. The dimensions of crystallites in $c$ direction were found from the formula: $L_c = 0.94\lambda/\beta_{002} \times \cos \theta$, where $\beta_{002}$ is angular half-width of (002) lines in radians.

Raman spectra were acquired by means of dispersion Raman microscope Senterra (Bruker), furnished with laser excitation at 785 nm; silicon CCD detector Idus (Andor), thermoelectrically cooled to −53°C. Spectra were recorded in optical geometry 180° in the range of Raman shifts 100–3200 $cm^{-1}$ at optical resolution of 3−5 $cm^{-1}$, using laser excitation power of 1–50 mW.

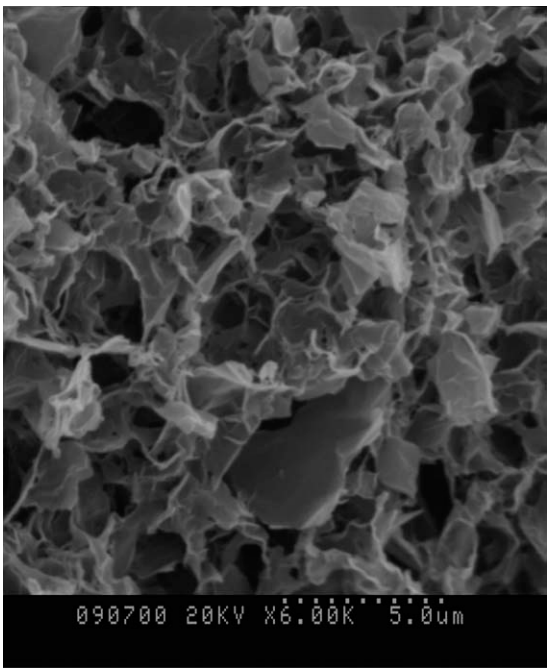


**Figure 1.** SEM microphotograph of pristine GNP powder.

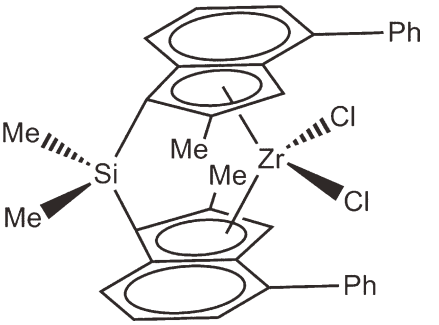


**Figure 2.** The structure of metallocene catalyst *rac*-$Me_2Si$(2-Me-4PhInd)$_2ZrCl_2$.

### Synthesis of Composites

Synthesis of composites was performed in liquid propylene in the presence of highly effective homogeneous catalytic system of ansa-zirconocene with $C_2$ symmetry type *rac*-$Me_2Si$ (2-Me-4PhInd)$_2ZrCl_2$ (MC), activated by methylaluminoxane (MAO) according to method, described in Ref. 9. The structure of catalyst is shown in Figure 2. This catalyst is characterized by high isospecificity and activity in propylene polymerization, yielding IPP with high molecular weight.[10]

Polymerization was carried out at 60°C and pressure ~ 2.5 MPa in a 200 $cm^3$ steel reactor, equipped with a high-speed stirrer (3000 rpm). Nanocomposites were prepared via two routes (in the second one the suspension of GNP was additionally sonicated for better dispersion): (1) the reactor was first filled with pristine graphene powder, preliminarily vacuum-processed at 200°C, then liquid propylene was introduced into reaction volume, followed by the necessary amount of MAO and metallocene catalyst; (2) suspension of graphene powder in toluene was sonicated for 0.5 h, then necessary amount of MAO was added and the mixture was additionally sonicated for 0.5 h. After that suspension was introduced in the reactor, filled with propylene, and then catalyst was finally injected. Concentration of filler in composite was controlled by varying the amount of filler, duration of polymerization and concentration of catalyst. Concentration of MC was (3–5) × $10^{-6}$ mole/L, the ratio Al/Zr was 13,000–15,000. Polymerization time was 15−30 min. The activity of metallocene catalytic system was equal to 50–100 $kg_{(PP)}$/($mmol_{(Zr)}$·h). Filler concentration in final composites varied from 0.05 to 5.6 vol %.

After polymerization, the composite powder was discharged from reactor and washed from the residuals of catalytic system in mixture of ethanol and HCl (10% solution), then repeatedly washed in ethyl alcohol and dried to constant weight in vacuum at 60°C.

### Characterization Methods

Infrared (IR) spectra of samples in the form of hot pressed films 100-$\mu$m thick were recorded using the method of frustrated total internal reflection (FTIR) with Vertex 70 FTIR Bruker spectrometer, equipped with diamond crystal single reflection GladiATR (Pike Technologies Inc.) accessory. Macrotacticity of PP was found from the ratio of the bands D998/D973. This

ratio characterizes the presence of isotactic sequences of propylene units consisting of more than 11–13 monomer units.[11]

Mechanical properties of composites (samples 0.5 × 5 × 35 mm) were tested with testing machine Instron 1122 at strain rate 50 mm/min and room temperature. Test specimen were cut from films, that were pressure molded at 190°C and pressure 10 MPa, cooling rate 16 K/min. The average values of mechanical properties were calculated from six tests for each concentration.

Transmission electron microphotographs of composites were taken with TEM microscope LEO-912 AB OMEGA (Germany) using accelerating voltage of 100 kV. Ultrathin sections of composite specimens with thickness of ~ 100 nm were prepared using a Reichert-Jung Ultracut ultramicrotome with diamond knife.

Thermophysical characteristics (temperature and enthalpy of melting and crystallization) of nanocomposites were investigated by differential scanning calorimetry (DSC) using Perkin-Elmer DSC-7 instrument at heating/cooling rate 10 K/min. Specific heat flow for melting peak was corrected for the mass of PP in nanocomposite. The results shown are for the second heating run.

Combustibility of composites was evaluated from Hot-wire ignition experiments. The specimens were wrapped with resistance wire that dissipated a specified level of electrical energy. The performance is expressed as the mean number of seconds needed to either ignite specimen or to burn through the specimen without ignition.

### Dielectric Measurements

The DC conductivity of the materials was measured by two-probe method at room temperature using disk electrodes. Dielectric properties of nanocomposites in microwave range (3.2–40 GHz) were measured by the cavity resonance method using KSVN R-2 standing wave instruments (Russia) with rectangular-shaped waveguides and resonators ($H_{01n}$ operating mode). The cavity resonance method is based on the determination of the shift of resonance frequency $\Delta f$ and the change of cavity $Q$ factor $(1/Q - 1/Q_0)$ when the sample is inserted into the cavity.[12] For example, at frequency 4.8 GHz $Q$ factor of the cavity was −20 dB; $Q$ factor of the cavity with sample inserted was −18/−10 dB, depending on dielectric losses of the sample. The measurements yield real ($\varepsilon$') and imaginary ($\varepsilon$") parts of nanocomposite permittivity. Samples for measurements were rectangular strips with typical dimensions 15 × 1 × 0.5 mm. Measurement error was 10% to 15%. Dielectric properties in frequency range 50–$10^6$ Hz were measured with the use of automatic digital LCR meter Fluke PM6306 on samples with silver-painted disc electrodes.

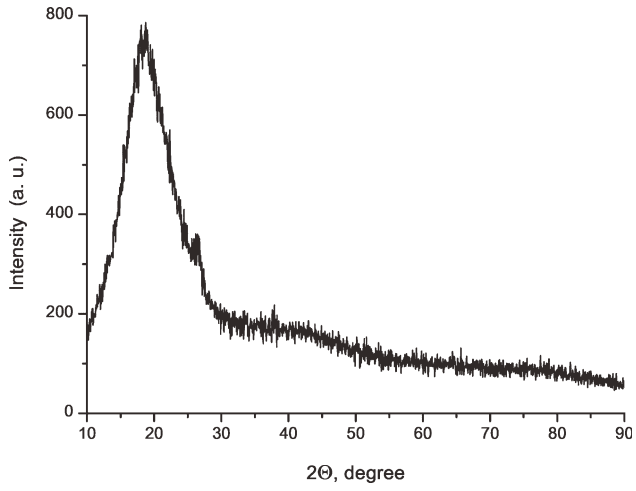


**Figure 3.** XRD pattern of GNP.

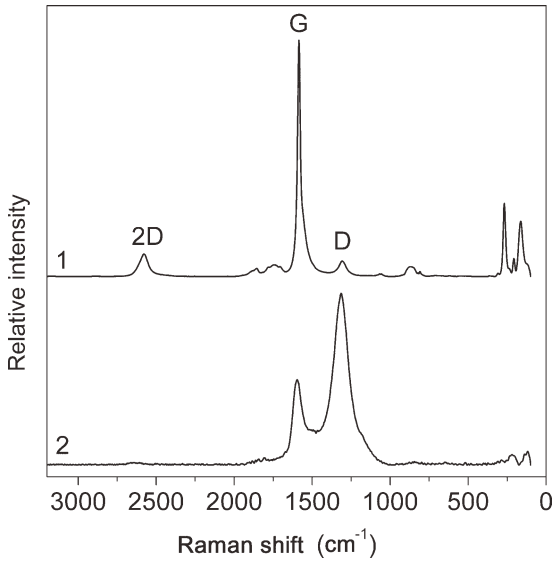


**Figure 4.** Raman spectra of MWCNT (1) and GNP (2). Spectra are vertically shifted for better comparison.

## RESULTS AND DISCUSSION

### Structure of GNP

X-ray phase analysis of GNP gives the parameters of crystal GNP in ***c*** direction: $d_{002} = 4.73$ Å, $L_c = 11.27$ Å, i.e., crystallites consist of 4 ± 1 layers of graphene. XRD pattern of GNP (Figure 3) shows trace amounts of other carbon allotropes, indicated by small peak at $2\Theta = 26$–$27°$.

Raman spectra allow estimating the ratio of ordered crystalline and disordered carbon structures in the material. Figure 4 compares Raman spectra of GNP and that of MWCNT.

The spectra show different ratio of intensities of the bands G/D for these materials. Band G in Raman spectra is usually assigned to phonon mode $E_{2g}$ of oscillations of $sp^2$-hybridized carbon atoms, bonded in condensed aromatic system (graphene plane), and called "order band," whereas band D is attributed to oscillations of $sp^3$- hybridized atoms and called "disorder band." It is currently recognized that high relative intensity of band D in Raman spectra of graphene (D-band at 1315 $cm^{-1}$ in Raman spectra of GNP) evidences essential reduction of the dimensions of regular (graphene) $sp^2$-domain planes—for example, as a result of extensive oxidation of graphite and subsequent reduction of graphite oxide, and also as a result of additional defects, introduced by exfoliation of graphite oxide during sonication.[13]

Applied Polymer SCIENCE

The ratio of intensities of the bands G/D in Raman spectra allows finding the dimension of crystallites in *a* direction, which turned out to be equal to 45 nm. Calculation were made using equation $L_a = 2.4 \times 10^{-10} \times \lambda^4 \times I_G/I_D$,[14] where $\lambda$ is laser wavelength in nm. That is, the ratio of crystallites size in directions *a* and *c* from Raman and X-ray data equals 40. Each graphene layer can be visualized as comparatively well-structured conjugated 2D polymer of molecular weight ~ 700 kDa, which acts as a short-range order center of structurization for nearby polyolefine chains.Comparison of frequencies of G-bands in Raman spectra of single-walled CNT "HIPCO",[15] MWCNT[3] and GNP is presented in Figure 5. Our data are in good agreement with dependence of G-band frequency on the number of layers in carbon particles,[16] also indicating that GNP used in this work is essentially 3–5 layer graphene. This is also confirmed by the presence of Raman-mode C peaks in the envelope of GNP G-band at 1586.5 $cm^{-1}$, characteristic of single-walled CNT or monolayer graphene, and also the contribution at frequencies 1584–1583 $cm^{-1}$, characteristic of 2–4 layer graphene particles. As to higher frequency components, specifically at 1597, 1607, and 1617 $cm^{-1}$, their origin is related to the presence of structural defects inside graphene layer, leading to the process of double Raman resonance and appearance of a shoulder in G-band at 1605–1620 $cm^{-1}$ (so-called $D^1$-band).[17] $D^1$-band is not visible in Raman spectra of comparatively low-defect single-walled (HIPCO) or double-walled CNT, but is invariably present in G-band of Raman spectra of solid graphite or graphene platelets, prepared by reduction of graphite oxide with hydrazine-hydrate. Summarizing X-ray and spectroscopy data, GNP were 2–4 layer graphene particles, ~ 45 nm long in plane direction and the aspect ratio (length to thickness ratio) of 40.

### TEM of Composites and Tacticity of Matrix Polymer

Figure 6 shows typical TEM images of the composites with pristine GNP (a) and sonicated GNP (b). It can be seen that in composites synthesized with pristine GNP, nanofiller particles form long thin aggregates, while sonicated GNP particles are uniformly distributed in polymer matrix in the form of smaller size anisotropic aggregates.

Raman microscopy spectra of a film of composite contain bands, specific both to GNP and matrix polymer (Figure 7). Relatively low intensity of IPP bands in composite with 0.05% vol GNP results from the fact that GNP, as well as other materials with extended conjugation system demonstrate resonance-enhanced Raman scattering under laser excitation of 785 nm, while IPP, devoid of conjugation, produces spontaneous spectrum, not enhanced by resonances. Resonance-enhanced Raman spectrum can be routinely 100–10,000 more intense, than spontaneous spectrum.

IR spectroscopy showed that the presence of filler in reaction system has no effect on stereospecificity of IPP, synthesized with the above catalytic system. Macrotacticity of polymer in composites was the same as for IPP, typically 82%–84%.

### Thermal Properties

DSC data for composites with pristine and sonicated GNP are listed in Table I. A slight increase of polymer melting point and enthalpy of melting is observed with increasing GNP content in composite.

The increase in crystallization temperature $T_{cr}$ is observed for both pristine and sonicated GNP, suggesting that, similar to previously reported data for MWCNT,[4] GNP is a nucleating agent for PP crystallization. The data of Table I and Figure 8

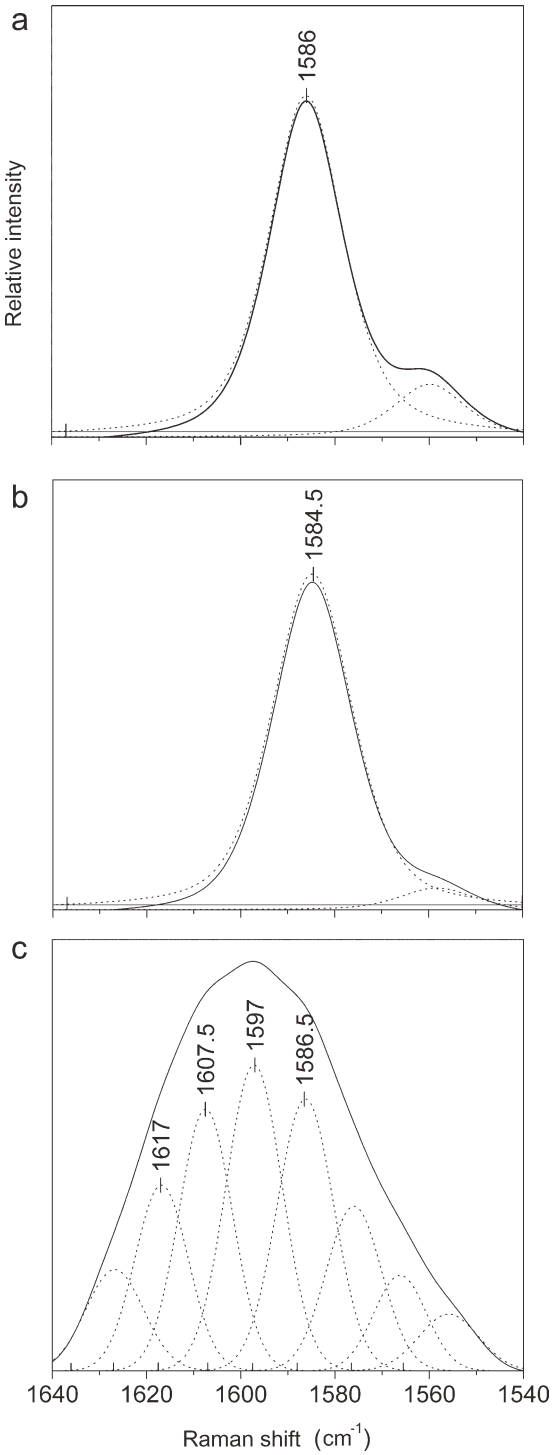


**Figure 5.** Comparison of G-band frequencies in Raman spectra of (a) single-walled CNT "HIPCO",[12] (b) MWCNT,[3] and (c) GNP of this work.

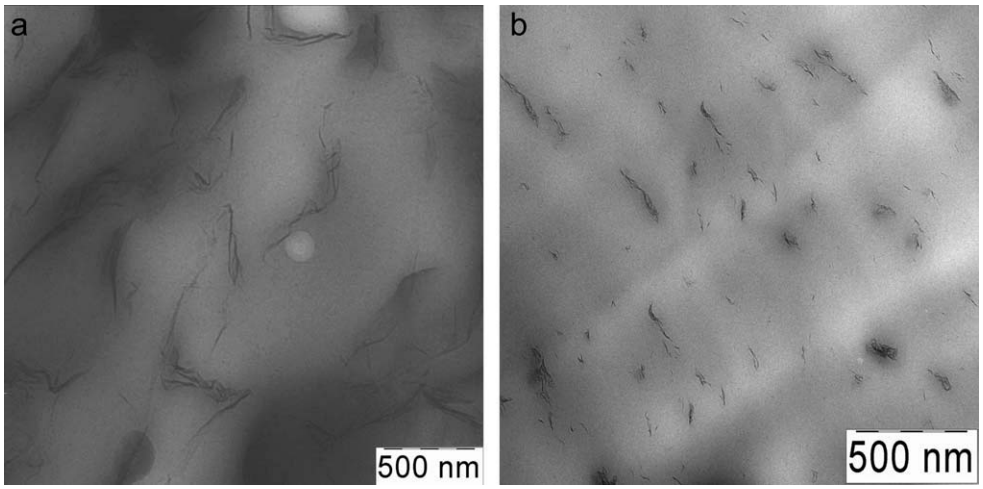


**Figure 6.** TEM microphotographs of composites with pristine GNP: 1.1 vol % (a) and sonicated GNP: 0.9 vol % (b).

show that this effect is more pronounced in the case of composites with sonicated GNP. This is probably explained by larger specific surface of ultrasonically treated particles inside the composite. The nucleating effect of small particles on IPP morphology results in smaller spherulites in polymer.

Composite samples with GNP and MWCNT have been tested by Hot Wire Ignition method, simulating thermal strains which can be invoked by the source of heat or ignition. It was found that the induction time of ignition of composites is essentially longer in comparison with pure polymer, illustrating lower combustibility of these materials.

### Mechanical Properties

Tensile mechanical properties of composites were performed in quasi-static deformation regime. Stress–strain curves gave the values of elastic modulus $E$, tensile yield strength $\sigma_y$, as well as tensile strength $\sigma_b$ and elongation at break $\varepsilon_b$. Mechanical properties of "metallocene" IPP are as: $E = 1200$ MPa, $\sigma_y = 36$ MPa, $\sigma_b = 40$ MPa, $\varepsilon_b = 540\%$. Composites with both pristine and sonicated GNP show increasing elastic modulus with increasing concentration of filler, and this is accompanied by sharp decrease of their deformation properties. Yield strength of composites with pristine GNP slightly decreases with increasing filler loading (from 36 to 34 MPa). The behavior of composites with sonicated GNP is different–yield strength is practically independent of filler concentration ($\sim$ 36 MPa), which probably indicates higher interphase energy at filler–matrix interface.

The dependence of relative elastic modulus $E/E_0$ and relative elongation at break $\varepsilon/\varepsilon_0$ on filler concentration for composites with sonicated GNP in comparison with MWCT are presented in Figure 9. The elastic modulus of composites is 25%–35% higher compared with that of the matrix. Composites with sonicated GNP seem to be more elastic than composites with MWCNT, i.e., in the former case elasticity is retained at higher concentration of nanocarbon filler.

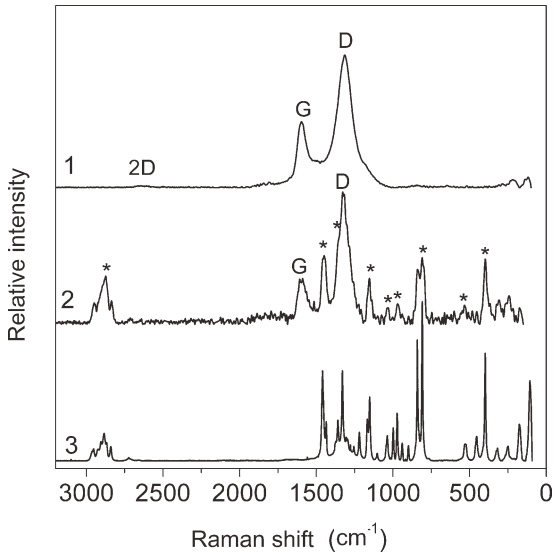


**Figure 7.** Raman spectra of GNP (1), composite with 0.05 vol % GNP (2), and pure IPP (3). Spectra are shifted along $y$-axis of ordinates for illustrative reasons. Asterisks in the spectrum of composite mark Raman modes of IPP matrix.

**Table I.** Melting Point ($T_m$), Enthalpy of Melting ($\Delta H_m$), Crystallization Temperatures ($T_{cr}$), and Enthalpy of Crystallization ($\Delta H_{cr}$) of Composites IPP/GNP

| Concentration of GNP in composite (vol %) | $T_{cr}$ (°C) | $\Delta H_{cr}$ (J/g) | $T_m$ (°C) | $\Delta H_m$ (J/g) |
|---|---|---|---|---|
| IPP | 105.5 | 102.0 | 154.6 | 100.8 |
| IPP/pristine GNP | | | | |
| 0.05 | 107.8 | 97.3 | 157.9 | 99.2 |
| 0.3 | 110.8 | 96.7 | 158.6 | 99.6 |
| 2.5 | 117.7 | 91.4 | 155.5 | 101.8 |
| IPP/sonicated GNP | | | | |
| 0.1 | 113.5 | 92.2 | 156.4 | 106.2 |
| 1.3 | 122.5 | 92.8 | 157.8 | 95.5 |
| 5.6 | 123.4 | 92.9 | 158.3 | 108.0 |

Applied Polymer SCIENCE

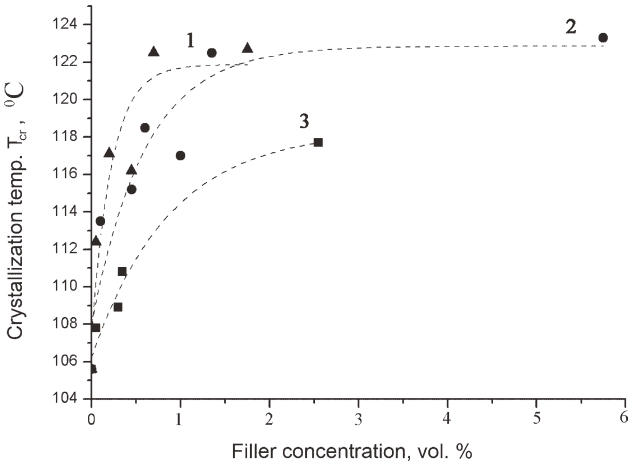


**Figure 8.** Crystallization temperature of IPP composites with carbon nanofillers. (1) MWCNT, (2) sonicated GNP, and (3) pristine GNP.

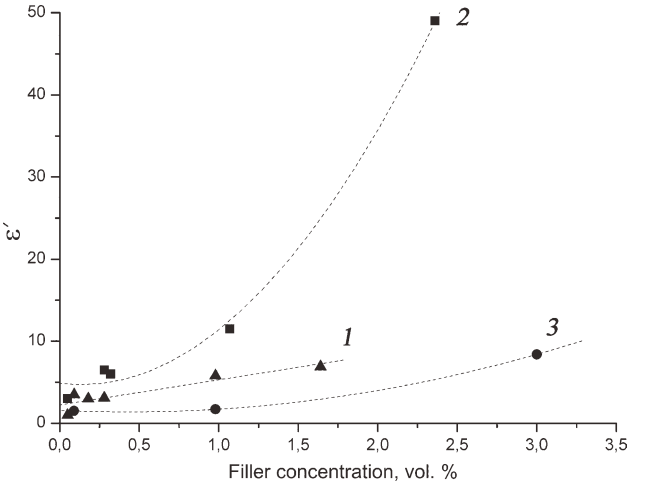


**Figure 10.** Dependence of dielectric permittivity on filler concentration. Frequency 4.8 GHz. (1) MWCNT; (2) pristine GNP; (3) sonicated GNP.

### Electrophysical Properties

DC electrical conductivity $\sigma_{DC}$ and dielectric properties at low frequencies ($10^2$–$10^6$ c/s), and in microwave range ($3 \times 10^9$ to $3 \times 10^{10}$ c/s) were studied as a function of filler content. Composites IPP/GNP showed high dielectric permittivity and losses in microwave range. Dielectric permittivity ($\varepsilon'$) increases sharply with increasing filler content, which apparently is caused by high interface surface in composites. The values of permittivity

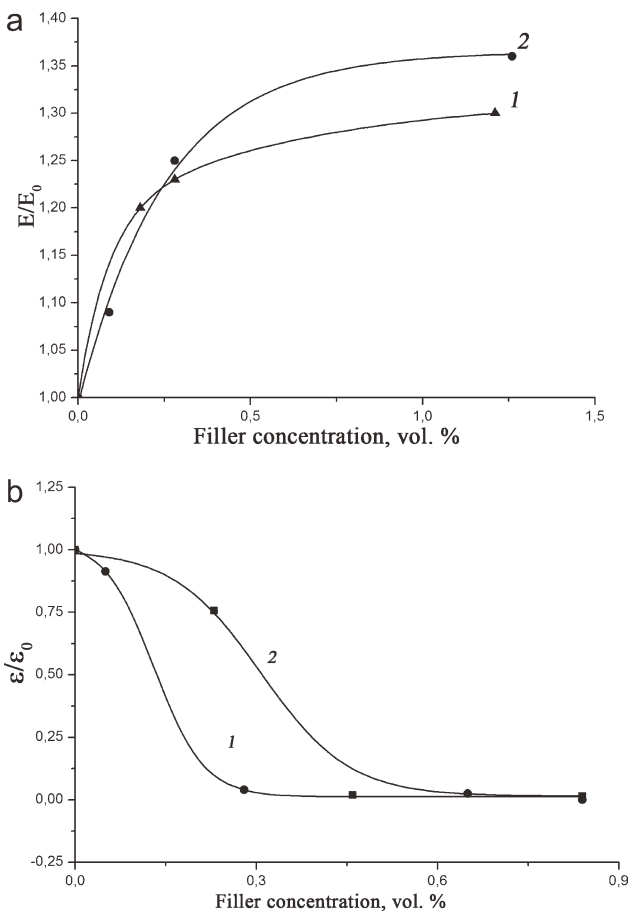


**Figure 9.** Dependence of relative elastic modulus (a) and relative elongation at break (b) on filler concentration. (1) IPP/MWCNT, (2) IPP/sonicated GNP.

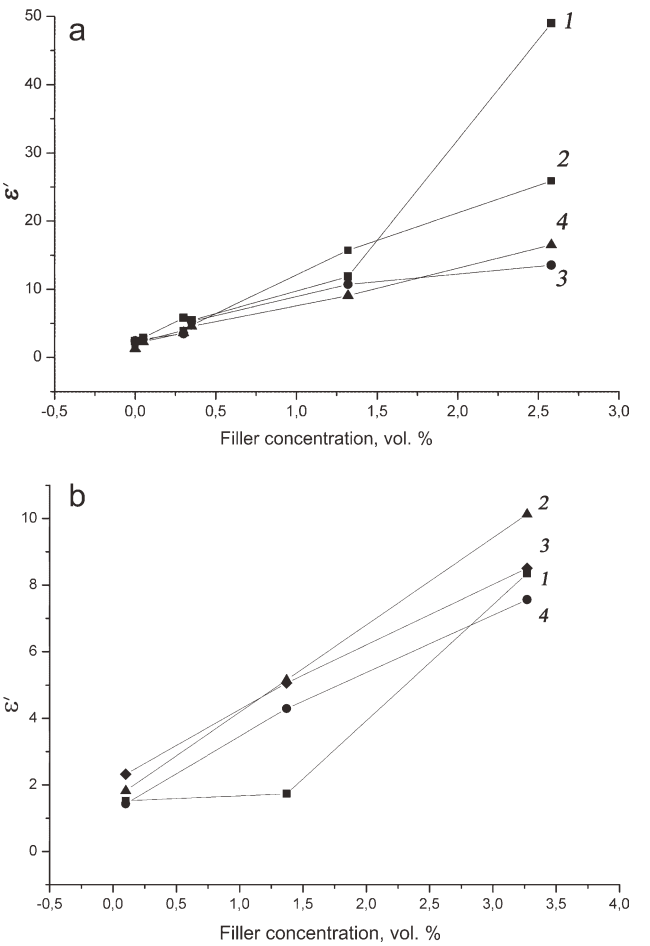


**Figure 11.** Concentration dependence of dielectric permittivity at different frequencies (1–3.2 GHz, 2–4.8 GHz, 3–6.6 GHz, 4–11 GHz): (a) composites with pristine GNP; (b) composites with sonicated GNP.

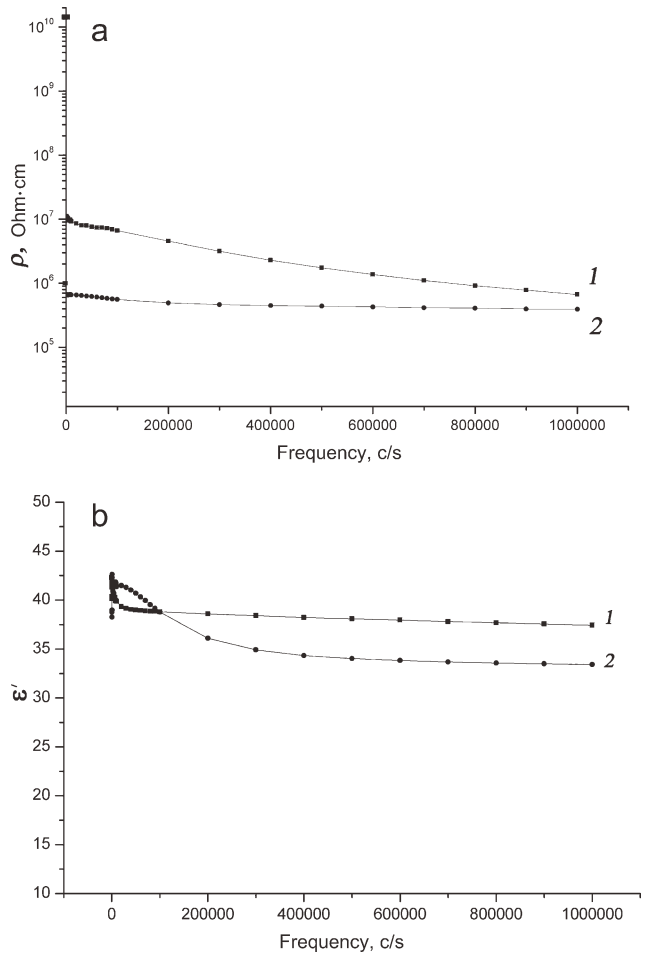


**Figure 12.** Dependence of AC resistivity and permittivity on frequency. Concentration of GNP in composite: 1–2.9 vol %, 2–5.6 vol %.

are much higher, compared with composites with MWCNT at similar concentration (Figure 10). Dielectric loss tangents tan $\delta$ varied typically in the range 0.01–0.5, depending on filler concentration.

Sonication of GNP powder was found to essentially affect dielectric permittivity and its dependence on concentration of GNP (Figure 11)–dielectric permittivity of composites with sonicated GNP is much lower, than composites with pristine GNP. Dependences of $\varepsilon'$ on concentration of GNP were analyzed using the mathematical model developed by authors.[4,5] This model allows to calculate the aspect ratio of conducting particles (or aggregates) in the form they are present in composite. Calculations have shown that the aspect ratio (characteristic ratio) for GNP particles in composite is equal to 77, whereas for MWCNT it is much lower and equals 25. Comparison with X-ray phase analysis data for pristine GNP particles indicates that GNP is present in composite as thin flaky aggregates of individual particles. Sonication was found to decrease the aspect ratio of these aggregates in composite to 31. Different aspect ratio, found for sonicated particles seems to be the primary factor, affecting the properties of composites.

Polymer composites with graphene sometimes exhibit low values of percolation threshold $v_{fc}$, i.e., concentration of filler $v_f$ where sharp increase of electrical conductivity occurs.[18] For example, composites of graphene in epoxy polymer have $v_{fc}$ = 0.52 vol %,[17,18] composites of graphene, prepared via polystyrene solution in dimethyl formamide have $v_{fc}$ = 0.1 vol %.[19] In composites of PP and pristine GNP, appreciable electrical conductivity of $1.9 \times 10^{-7}(\Omega\ \mathrm{cm})^{-1}$ was found at filler concentration 2.4 vol %. Composites with sonicated GNP have electrical conductivity $1.5 \times 10^{-10}$ and $1 \times 10^{-6}$ $(\Omega\ \mathrm{cm})^{-1}$ at filler content 2.9 and 5.6 vol %, accordingly. This means that the value of percolation threshold is below 2–3 vol %, much lower compared with *in situ* polymerized IPP with graphite.[9] Apparently, the method of *in situ* polymerization forms a layer of polymer layer on the surface of particles or aggregates of filler particles, which hinders contacts between them and blocks the formation of conductive cluster in composite.

Both electrical conductivity (resistivity) and dielectric permittivity of composites with filler content 2.9 and 5.6 vol %, weakly depend on frequency in the range 50–$10^6$ Hz (Figure 12),

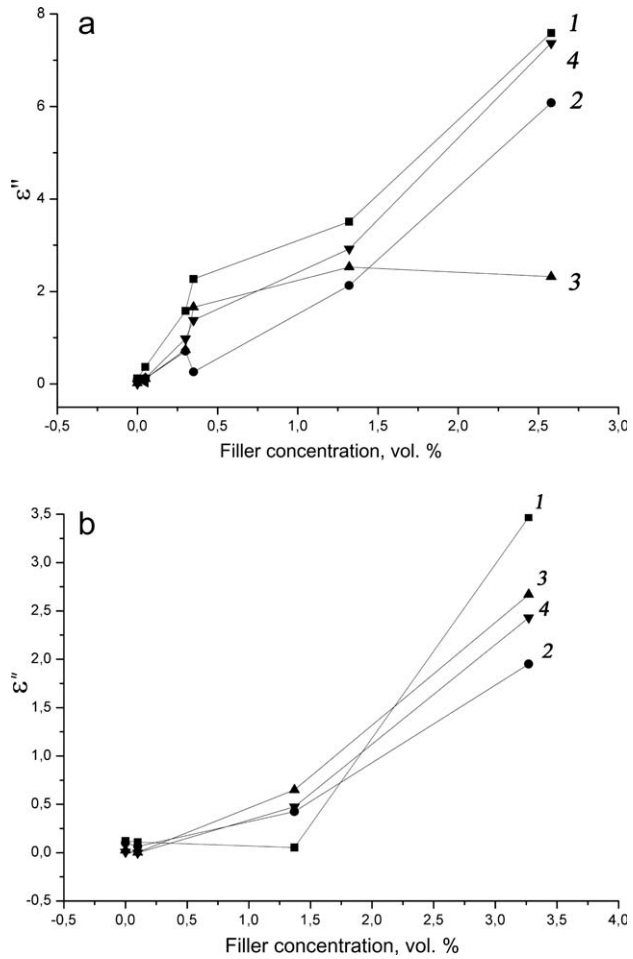


**Figure 13.** Concentration dependence of dielectric losses at different frequencies (1–3.2 GHz, 2–4.8 GHz, 3–6.6 GHz, 4–11 GHz): (a) composites with pristine GNP; (b) composites with sonicated GNP.

indicating that concentration of GNP is above percolation threshold.

Both MWCNT and GNP possess high electrical conductivity, making it possible for polymer composites to absorb high-frequency electromagnetic radiation. The important factor is that the percolation threshold is rather high for *in situ* polymerized composites, so that high local electrical conductivity is combined with no appreciable bulk conductivity. This results in a considerable increase of dielectric losses (Figure 13), while permittivity remains much less, than could be in the presence of bulk conductivity. The combination of these two factors is favorable for reducing reflection of electromagnetic radiation and increasing its absorption.

## CONCLUSION

The results of investigations clearly show that carbon nanosized fillers can be successfully used to modify the properties of PP. The ratio of nanoplatelets, the filler nanoparticles, size in two directions equals 40 from Raman and X-ray data. The aspect ratio for GNP particles aggregates in composite is equal to 77. Comparison with X-ray phase analysis data indicates that GNP is present in composite as thin flaky particles aggregates. Sonication was found to decrease the aspect ratio of GNP particles aggregates in composite to 31. IR spectroscopy showed that the presence of filler in reaction system has no effect on stereospecificity of IPP. Crystallization temperature of PP increases in composites with both pristine and sonicated GNP. The composites have useful dielectric properties, low combustibility, enhanced crystallization temperature, and elastic modulus. Composites with both pristine and sonicated GNP show increasing elastic modulus with increasing concentration of filler, and this is accompanied by sharp decrease of their deformation properties. Comparatively low values of permittivity and high dielectric losses in microwave range indicate that they can be used as screens and filters of electromagnetic radiation, or as semiconducting layers in power cables.[20,21]

## ACKNOWLEDGMENTS

The authors thank Dr. Sergey S. Abramchuk from Moscow State University for his invaluable assistance in transmission electron microscopy analysis.

## REFERENCES

1. Novoselov, K. S.; Geim, A. K.; Morozov, S. V.; Jiang, D.; Zhang, Y.; Dubonos, S. V.; Grigorieva, I. V.; Firsov, A. A. *Science* **2004,** *306*, 666.
2. Kim, H.; Abdala, A. A.; Macosco, C. *Macromolecules* **2010,** *43*, 6515.
3. Verdejo, R.; Mar Bernal, M.; Romasanta, L. J.; Lopez-Manchado, M. A. *J. Mater. Chem.* **2011,** *21*, 3301.
4. Koval'chuk, A. A.; Shchegolikhin, A. N.; Shevchenko, V. G.; Nedorezova, P. M.; Klyamkina, A. N.; Aladyshev, A. M. *Macromolecules* **2008,** *41*, 3149.
5. Kovalchuk, A. A.; Shevchenko, V. G.; Shchegolikhin, A. N.; Nedorezova, P. M.; Klyamkina, A. N.; Aladyshev, A. M. *J. Mater. Sci.* **2008,** *43*, 7132.
6. Stankovich, S.; Piner, R. D.; Chen, X.; Wu, N.; Nguyen, S.-B. T.; Ruoff, R. S. *J. Mater. Chem.* **2006,** *16*, 155.
7. Hummers, W.; Offeman, R. *J. Am. Chem. Soc.* **1958,** *80*, 1339.
8. Muradyan, V. E.; Romanova, V. S.; Moravsky, A. P.; Parnes, Z. N.; Novikov, Yu. N. *Russ. Chem. Bull.* **2000,** *49*, 1017.
9. Nedorezova, P. M.; Shevchenko, V. G.; Shchegolikhin, A. N.; Tsvetkova, V. I.; Korolev, Yu. M. *Polym. Sci. Ser. A* **2004,** *46*, 242.
10. Spaleck, W.; Kuber, F.; Winter, A.; Rohrmann, J.; Bochmann, B.; Antberg, M.; Dolle, V.; Paulus, E. F. *Organometallics* **1994,** *13*, 954.
11. Kissin, Yu. V. Isospecific Polymerization of Olefins; Springer-Verlag: New York, Berlin, Heidelberg, Tokyo, **1985.**
12. Apletalin, N.; Djakonova, O. A.; Kazantsev, Y. N.; Simonyan, D. E.; Solosin, V. S.; Zubov, A. S. In: Abstracts 3rd International Conference "Electromagnetism in Aerospace Applications"; Torino, Italy, **1993,** p 253.
13. Zhao, X.; Zhang, Q.; Chen, D.; Lu, P. *Macromolecules* **2010,** *43*, 2357.
14. Pimenta, M. A.; Dresselhaus, G.; Dresselhaus, M. S.; Cançado, L. G., Jorio, A.; Saito, R. *Phys. Chem. Chem. Phys.* **2007,** *9*, 1276.
15. Lobach, A. S.; Solomentsev, V. V.; Obraztsova, E. D.; Shchegolikhin, A. N.; Sokolov, V. I. *AIP Conf. Proc.* **2004,** *723*, 209.
16. Wang, H.; Wang, Y.; Cao, X.; Feng, M.; Lan, G. *J. Raman Spectrosc.* **2009,** *40*, 1791.
17. Ferrari, A. C. *Solid State Commun.* **2007,** *143*, 47.
18. Li, J.; Kim, J.-K. *Composites Sci. Technol.* **2007,** *67*, 2114.
19. Li, J.; Vaisman, L.; Marom, G.; Kim, J.-K. *Carbon* **2007,** *45*, 744.
20. Spitalsky, Z.; Tasis, D.; Papagelis, K.; Galiotis, C. *Progr. Polym. Sci.* **2010,** *35*, 357.
21. Kim, J.-B.; Lee, S.-K.; Kim, Ch.-G. *Key Eng. Mater.* **2007,** *334-335*, 837.